



LIGHTWEIGHT STRUCTURES IN CIVIL ENGINEERING CONTEMPORARY PROBLEMS

INTERNATIONAL SEMINAR
Organized by Polish Chapters of
International Association for Shell and Spatial Structures
Rzeszów University of Technology, Faculty of Civil and
Environmental Engineering and Architecture
XXI LSCE –2015

Rzeszów, 4 December, 2015 (Friday)

Above lines and symbols will be printed by publisher



Structural analysis of long-span trusses of a speedway stadium roof

J. Szafran¹⁾ A. Nowakowski²⁾

¹⁾ Adjunct Professor, Chair of Structural Safety, Department of Structural Mechanics, Faculty of Civil Engineering, Architecture and Environmental Engineering, Technical University of Lodz, Łódź, POLAND,
email: jacek.szafran@p.lodz.pl

²⁾ M.Sc. Engineer, Faculty of Civil Engineering, Architecture and Environmental Engineering, Technical University of Lodz, Łódź, POLAND

ABSTRACT: The main aim of this article is a global, conceptual analysis of a speedway stadium which is an adaptation of an existing sports object: Beira Rio in Porto Alegre. The following elaboration includes a selection process of the primary elements' geometries for the concerned structure: truss girders, and presentation of geometric parameters for the whole cover area. The results were obtained from two analyses conducted on two individual computational models (a model of a single girder and of the whole structure) which have been later compared. The load induced by climate was estimated with methods approximating its real distribution, based on standards in force. The impact of susceptibility coefficient for soil (at the location of the object) on displacements and stress in structure's elements has been analyzed. In order to obtain reliable results, an analysis of the whole object has been conducted. It took stiffness of particular elements and their mating into account which could not have been determined without a spatial model because of the structure's complexity.

Keywords: roof trusses, global analysis, wind load, design process, coefficient of soil reaction

1. INTRODUCTION

Erecting sport facility structures has always posed serious challenges to the architects and the constructors. On one hand, their size is enormous; on the other, their supporting structures are often avoided as they significantly limit the visibility of the spectacle. Apart from that, the current sporting objects design trends place the comfort and the safety of the spectators [2, 3], first compromising the aforementioned unreduced visibility of the show. Last but not least, the protection from unfavourable weather conditions is another aspect that has to be considered.

The design of the structure should also convey a specific impression and style, leading to more and more interesting architectural shapes which aesthetically enrich the show but unfortunately further increase the complexity level of the structure. Nevertheless, the appearance of the object is deemed equally important to the demanding audience of the current times and has to be considered.

It is therefore essential to design so-called long span roofs which exploit the state of the art technologies and design approaches allowing for deadweight reduction while maintaining the carrying capacity characteristics. The essential challenge of light roof design is the fact that as weight of a roof decreases, susceptibility to wind action increases leading to the elevation of the structure. Therefore the wind load on the object has to be assessed with high precision, which is often one of the most difficult phases in the design of the roof; a nonstandard structure shape is a frequent cause for such difficulties.

On the other hand, aspects that undoubtedly have to be taken into consideration are economic criteria for a project. While the erected objects are getting larger and more complex, requiring cutting edge design approaches, they generate enormous construction and building costs. In those types of structures, it used to be material weight that was

the most popular criteria as far as the budget was taken into consideration. Nowadays, it is rather complex installation and production of materials that are both lightweight and high strength like technical fabrics, which is becoming important economically.

It is extremely relevant to select an appropriate structure type at the design stage to reap benefits at the strengths of the chosen load-carrying system. Currently a few basic types of load carrying structures are available, which are applied according with assumptions made for object's dimensions, functional requirements, or aesthetics. They are predominantly based on frame systems (simple truss girders), or arcs systems (masts or tension rods), or other structural systems.

2. BEIRA RIO STADIUM AS INSPIRATION

The authors decided for an attempt at structural solutions adaptation of Beira Rio stadium especially when the stands area cover of the conceptual object is concerned. The stadium was deemed appropriate not only for its interesting architecture, but also challenges that are presented to the designer by response analysis of such a complex shape. The stadium in Porto Alegre was build along preparation for 2014 FIFA World Cup which was held in Brasil. It is a property of local football club Sport Club International which encouraged cooperation with architectural design studio, Hype Studio Architecture, to create a new design of the stadium. The object had to provide an entire level of corporate suites, as well as new VIP and lounge areas. Those features promised a stadium of XXI century which would be modern, comfortable, and safe. From the architectonic point of view, the building's roof consisted of curved truss girders which resembled a leaf. The visualization of the object taken by the Authors of the original project is presented in Fig. 1.

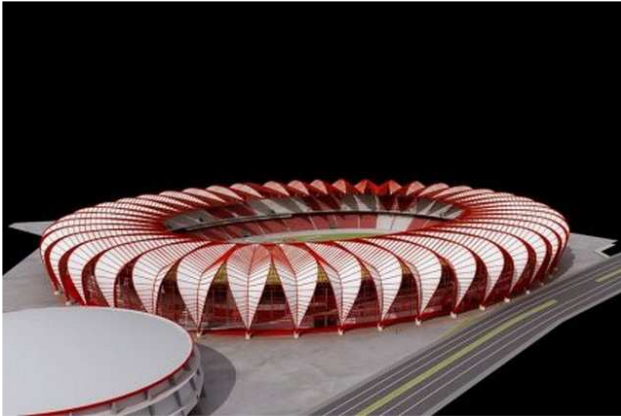


Fig. 1. Conceptual roof visualization of Beira Rio stadium (source: www.hypestudio.com.br).

The new steel roof cover is a modular structure consisting of sixty five curved truss girders accommodated around stands of oval size. They are overhang at 45 meters above the stadium's pitch. The roofing was constructed using PTFE membrane (Teflon fabric) stretched over a system of short rods arranged along the upper and bottom curves of the girders. The girders are part of a cantilever structure along with foundation support structures at their articulated joints and auxiliary, indirect, double-point support in the form of two-branch steel mullions. Such a system provides the girders with support along both horizontal and vertical directions. Furthermore, seven circumferential beam rings which connect bottom girder lines were utilized, and play a role of spring load support allowing for mechanical girder mating due to circumferential forces. A working platform and light and sound systems were attached to a ring that can be identified at the inner edge of the roof. It is a spatial lattice structure of a triangular cross-section.

3. THE OBJECT'S STRUCTURE

3.1. Selection of the roof's shape

Speedway tracks have characteristic, oval shape consisting of two straights and two arcs. The length to width ratio of outer track contour is approximately 2 to 1. Such a geometry determines the shape of the stands and the roof at the same time. In practice, the inner contour of the roof corresponds to the outer contour of the track for every roofed speedway stadium in the world. Therefore the use of cantilever structures seems most logical as their main bearing elements can be arranged around an oval shape of great length.

As mentioned in point 2, it was decided for an adaptation attempt at a structure which combines cantilever and structural systems used at Beira Rio stadium providing cover for both the stands and the track. Such a solution, to knowledge of the authors, has never been implemented in practice. Whereas the only stadium with cover for both stands and tracks is Motoarena Toruń, it implements solely bracket system.

In view of the cantilever structural system selected for the model, its geometry has to be a spatial system with element mating that would provide object's stability. If a traditional bearing girders system is used, that is placing the elements along the oval track line; it becomes impossible to have a coherent structure with a shape that efficiently transfers loads because forces perpendicular to its long straight elements would induce considerable displacement into the interior of the structure because of object's low spatial stiffness. An ideal shape would be spherical (the most energetically beneficial shape) or an arc, which would provide greater stiffness. It can be explained using a simple comparison of ring displacements: round, elliptic, and oval. Fig 2 presents displacements for three flat bar systems:

- a circle of a 5 m radius
- an ellipse of 2.5 m and 5.0 m axes
- an oval of circular arc radiuses equal to 2.5 m and lengths of straight lines of 5.0 m.

The geometry of the objects was selected so that their greatest dimensions were equal (both the ellipse and the oval can be inscribed in the circle). For an appropriate comparison of ring displacements, the bars which form the structures have equal diameters and stiffness modules. Moreover, the applied, linear, constant load of 10 kN/m is equal for each object and directed towards their interiors. Four mobile supporting structures were added that allow for free displacement within the models.

The conducted calculations indicate that the circle practically was not subjected to displacements. In case of uniform load by external pressure, a round body responds best as the particles aim at getting the least energy possible, a circle is a shape that, taken the surface it limits, has the least perimeter possible.

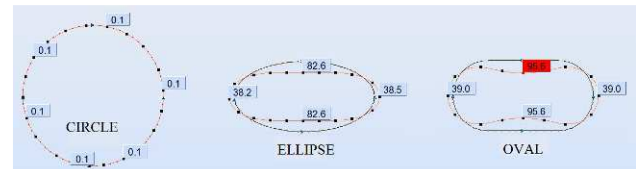


Fig. 2. Displacement of the rings: circular, elliptic, and oval with uniform load of 10 kN/m directed inside.

The oval ring experiences significant displacement (95.6 cm) in direction perpendicular to its straight lines, which confirms the unfavourable geometry of this object as far as the spatial stiffness, is taken into consideration.

Ellipse presents a compromise between circular and oval shapes. With the geometry similar to the one of the oval, it results in higher stiffness of the object. The elliptical ring experiences nearly 14% less displacement than the oval one as shown in the conducted numerical analysis. Its greatest displacement was 82.6 cm.

The analysis has pointed out the fact that an ellipsis is the most beneficial if its ratio of semi-minor to semi-major axes is as close to one as possible, and its shape is similar to track's geometry. When selecting geometric features of the analysed object, it was therefore decided to follow this guideline, assuming an elliptical shape of the plan and parameters determined by the tracks and the stands.

3.1.1 Data concerning the tracks

General assumptions concerning dimensions of the tracks, their surroundings, and the stands have been made in order to select the geometry of the structure. The following parameters of the tracks were assumed based on guidelines of Federation of International Motorcycling [6]:

- the Total length measured at 1.0 m from the internal contour: 345.0 m,
- the lengths of the straights: 75.0m,
- the width of the straights: 10.0 m,
- the width of the arcs: 10.0 m,
- the internal dimensions of the tracks: 70.0 x 160.0.

Moreover it was assumed that inflated barriers of 1.0 m width would be installed around the tracks and 2.5 m safety zone would separate the stands from the tracks.

3.1.2 Cover and stands data

A general architectonic draft of the stands was created based on [8] and [9]. The works require that the stands are designed in such a way as to provide enough visibility of the show for every spectator as well as security and comfort of mobility across the object. It was to be achieved by following the recommendations for dimensions concerning, e.g., seats. Moreover, according to guidelines [6], the angle of inclination of the stands should not be greater than 35°. Following the standards, the parameters of the stands were set:

- type of seats: single
- seats number: about 25,000
- width of a single seat: 0.50 m
- depth of a seat: 0.35 m
- stairs width: 0.75 m

- width of passages between rows: 0.40 m
- Inclination angle of the stands: 33°
- Maximum stands' height: 22.5 m
- The widths of the stands were correspondingly: minimum was 17.0 m, maximum was 30.6 m

The required area of the roof is about 50 m according to the fact that it should cover both the stands and the track. To provide cover for the whole required surface, the following parameters of ellipsis were chosen: the external ellipse, constituting an axis for girder locations, had dimensions A=76.0 m, B=104.0 m, and the internal ellipse constituting the axis of the internal ring had A=24.0 m and B=52.5 m.

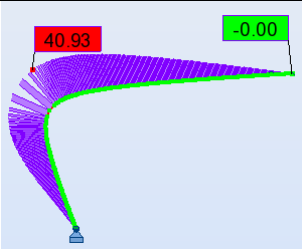
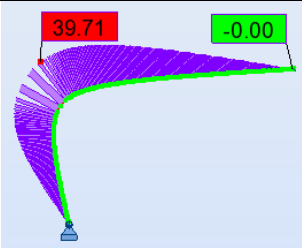
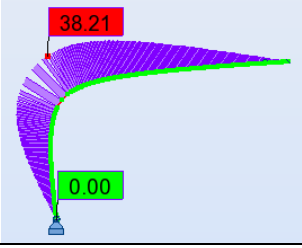
3.2. Selection of bearing girders geometry

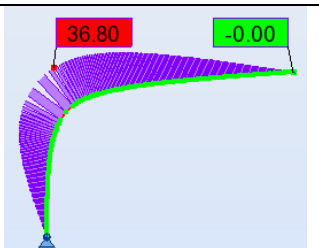
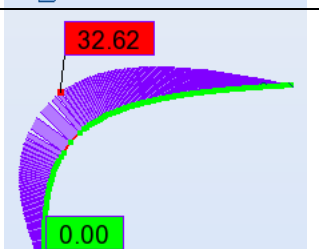
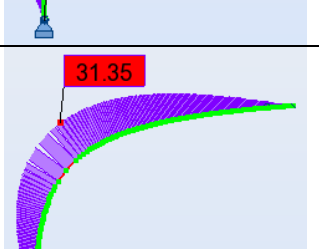
The selection of bearing girders' shape was the next step. In order to parameterize the structure, it was decided to use girders of a hyperbolic curve shape. In practice, however, it would be difficult to manufacture elements of hyperbolic curvature. On the other hand, in context of rapid advancements of automation techniques and Computer Aided Manufacturing (CAM) technology, it seems that this operation would be much easier.

Every girder consisted of bar elements: a bottom strap, two top straps and truss which connects the former with the latter.

In order to define the most beneficial hyperbole parameters, six comparable bar numerical models were created which correspond to the bottom girder strap. Each of them had a shape of a hyperbola section of various parameters.

Table 1. Analytical models parameters for the bottom straps and bottom hyperbolic girders with numerical calculations results.

Model number	Parameter [m]		Bending moments distribution (numerical analysis results)
	a	b	
1	10	7	
2	10	8	
3	10	9	

4	10	10	
5	30	24	
6	30	25	

The results above yield the following conclusions: hyperbolas of higher A and B parameters, and therefore lower curvature, allow for lower bending moments (with similar heights and reach). In case of hyperbolas of greatest curvatures (models no 1-4), an accumulation of bending moment can be observed in the fragment of the highest curvature. A negative result of the use of hyperbola of smaller curvature is the necessity for higher girders. For further analyses, the bottom girder strap geometry was assumed as in model no. 5. This way, the impact of accumulation of bending effects was limited and a satisfactory height of a girder was achieved (Fig. 3).

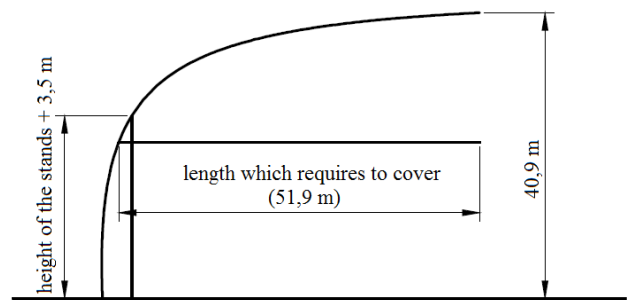


Fig. 3. Bottom girder strap geometry.

The next phase was a selection of top geometry straps, which assumed a shape of a hyperbola as well. The process was analogical to the bottom strap for this case, with an additional step consisting of a rotation of curves in relation to the surface (Fig. 4).

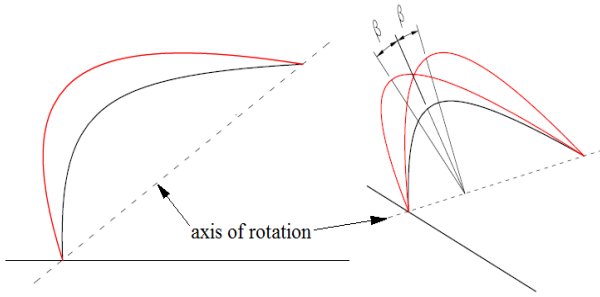


Fig.4. Rotation of top girder straps.

The main factor determining the curvature and the rotation angle of the surface of top straps was maximum length of the section perpendicular to both the bottom and the top strap. However, it should not have been too large because it would have been necessary to utilize long thin lattice bracing elements. It was finally decided for a hyperbola of the following parameters: $a = 130$, $b = 45$, and a rotation angle of $\beta = 10,78^\circ$. This way the resulting girder geometry determined the maximal theoretical length of lattice elements: 10.67 m (Fig. 5).

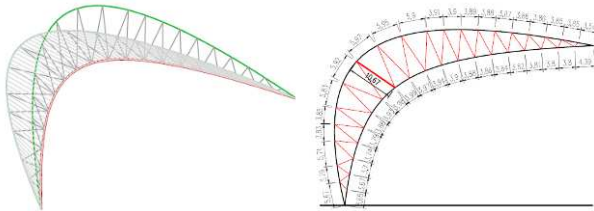


Fig. 5. Geometry of a girder with the view surface highlight.

3. Girders arrangement around the stadium stands

The girders were arranged between two ellipses (described in point 3.1.2) in such a way that the girder's plane was perpendicular to tangents of both curves at a support point of a girder, that is support points on fundamentals arranged around the ellipsis and the girder's node on the elliptical inner ring. In order to make the structure as repeatable as possible, the girders were arranged around the outer ellipsis at equal intervals (15.5 m) dividing its shape into 38 equal parts (Figs. 6-7). 38 bearing girders were effectually used.

As a result of the uniform distribution of bearing elements around the external ellipses, the set of girder nodes around the elliptic top ring became dense on the length of the most curvature. It may have been expected that an increase in internal forces of the ring would occur in these sections. On the other hand, its one positive effect for the whole structure would be an increase in its stiffness against loads perpendicular to the semi-major axis due to its tighter holding by the girders in the zones of more density, and consequently a decrease in ring displacement.

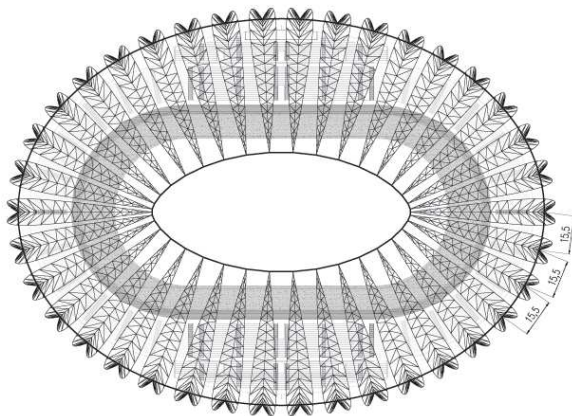


Fig. 6. Bearing girders arrangement – floor plan.

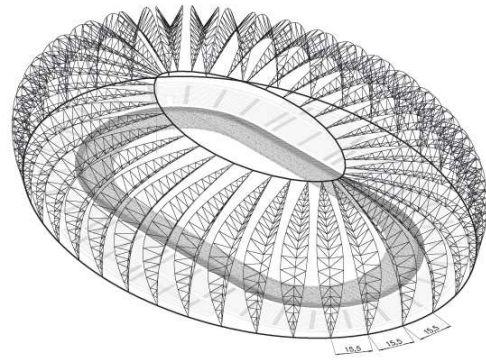


Fig. 7. Bearing girders arrangement - 3D view.

A graph below shows relation between modulus of elasticity for the supporting elements and ring's displacement: an increase in ellipsis support stiffness in zones of greater curvature decreases maximum displacement occurring perpendicularly to the semi-major axis. The decrease in the displacement slows down with the further increase in the elasticity modulus. The graph exhibits characteristics of hyperbolic function, which is confirmed in equation (1).

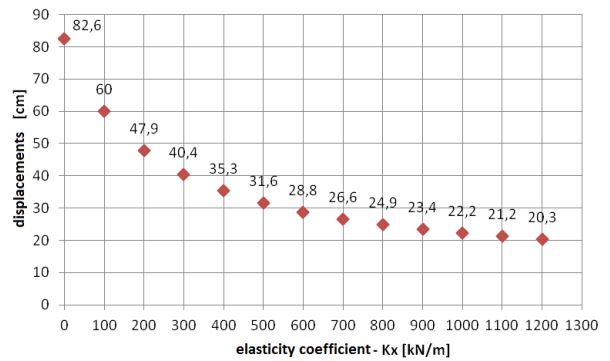


Fig. 8. The relation between maximum displacements of elliptic ring against elasticity modulus K_x .

$$K_x = \frac{F}{\delta} \left[\frac{kN}{m} \right], \quad (1)$$

After transformation:

$$\delta = \frac{F}{K_x} [m], \quad (2)$$

which yields an analogy to a basic hyperbolic relation:

$$y = \frac{a}{x}, \quad (3)$$

where:

K_x – modulus of elasticity,

F – force,

δ – displacements.

3.4. Cover of the structure

Taking Beira Rio stadium in Porto Alegre as a model, it was assumed that the structure would be covered with a technical fabric PTFE (Teflon) stretched between the girders' top straps and the bottom one's (Fig. 9), and its pressure action would be realized through a system of short rods arranged along the straps of a girder. A cover made with polycarbonate panels was assumed for surfaces between top straps of

neighbouring elements (Fig. 10), which would be attached to secondary structure bars on an appropriate aluminium frame.

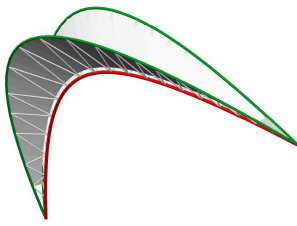


Fig. 9. Fabric cover on a girder.

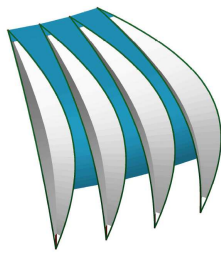


Fig. 10. Structure's cover of fabric (white) and panels (blue).

4. NUMERICAL MODELS OF THE STRUCTURE

Two three-dimensional, bar computational models were created for the purpose of comparative analysis:

- a model of the whole structure, and
- a model of a single girder (for the purpose of comparison).

The model of the whole structure allows for taking into account the stiffness impact of each of the elements on roof's response. In the second case, a single girder model, the authors attempted at estimation of support's susceptibility in order to represent the actual work manner of the system as accurately as possible. However, it should be noted that the more accurate idealization of the structure would be represented by the model of the whole structure.

4.1. Single girder computational model

A division of girder's straps into finite elements, at the stage of creating the model, allowed for an accurate determination of internal forces and structure's displacements while keeping the optimality of the model that relies on reduction in nodes and beams numbers.

In order to choose the best option, three models representing a bottom strap of the girder had been compared. They were divided into elements of lengths 0.5 m, 1.0 m, and 2.0 m. An element was assumed as circular, hollow section CHS 610x20 for the sake of the analysis. Axial forces incurred by the deadweight have been compared. The results of the analysis are presented in Tab. 2.

Table 2. Axial forces in the bottom strap against the number of finite elements.

Model	Finite element length [m]	Axial force [kN]	
		F_{max}	F_{min}
1	0,5	216,96	107,59
2	1,0	219,29	106,69
3	2,0	219,99	106,75

The differences between particular models are negligible and both allow for satisfactory approximation, so model 3 has been chosen for further analysis where the girder straps are divided into finite elements of a length of 2.0 m.

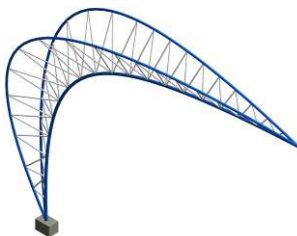


Fig. 11. Visualization of a steel structure of a girder.

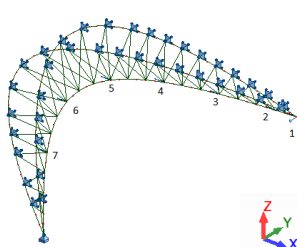


Fig. 12. Computational model of a girder.

Figure 11 and Figure 12 show visualisations and computational models for a single girder. The modelled supporting elements marked as flexible were numbered 1-7. Their parameters are presented in Tab. 4.

Table 4. Parameters of flexible supporting elements of a girder.

Element number	Applied force [kN]	Displacement [m]	Elasticity modulus in the given direction [kN/m]		
			X	Y	Z
1	1000	0,014	71428,57	fixed	0
2	100	0,061	1639,34	fixed	0
3	100	0,070	1428,57	fixed	0
4	100	0,079	1265,82	fixed	0
5	100	0,087	1149,43	fixed	0
6	100	0,094	1063,83	fixed	0
7	100	0,097	1030,93	fixed	0

A truss ring constitutes a supporting element for the girder. Its fragment was loaded with a horizontal force of 1000 kN directed towards the interior of the ring. A truss section consisting of two spans over three girders was deemed as representative. Its ends were articulated and the joints to which the girder was attached were supported in such a way that vertical displacement was blocked. The profiles of the truss straps were assumed as hollow circular CHS 508x20 and CHS 273x16, and the profiles of the truss elements (bars) were CHS 168,3x8. The displacements were determined during the numerical calculations which later yielded the susceptibility of the supporting structure (the analyzed section of the ring) using equation (1).

The susceptibility of the rings, of assumed circular diameter CGS 273x16, was analogically determined. Their supporting elements at the ends were fixed and accentuated, while the middle support was fixed only vertically. Each of the ring fragments was loaded with force equal to 100 kN at the central node, corresponding to the support point of the analyzed girder. The susceptibility of the rings supporting bottom strap of the girder was determined based on the displacements.

4.2. Roof structure computational model

Analytical model of the whole structure of the roof consists of 38 girders described in point 4.1 arranged between the elliptic external ring and the top truss one. It includes perimeter rings, bars connected to top straps of neighbouring girders, and also exhibits densities increasing spatial stiffness of the structure.

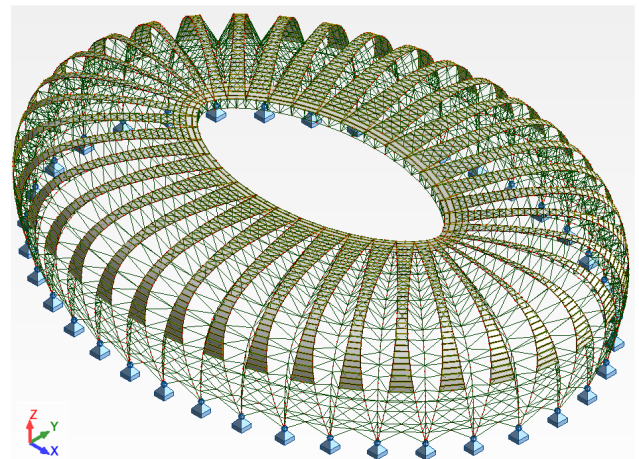


Fig. 13. Computational model of the roof structure.

Girder straps were modelled as beam elements, their connections with truss elements as stiff ones which results from the assumption that welding had been the attachment manner. The only elements of articulated nodes are the elements of the secondary structure, connecting top straps of the neighbouring girders, for which the node attachment manner is articulated and involves screws.

The height of the truss top ring was decided after numerical calculations had been performed for deadweight load and its maximum displacement was compared for various truss heights. One interesting relation was observed during the analysis. An increase in the distance between top and bottom straps caused a decrease in displacements. However, 3.5 m have been reached, the decrease got significantly smaller and further

increase in truss height caused only gradual increase in displacements. Finally the height of the truss was decided to be 3.5 m.

5. OBJECT'S LOAD STATE

5.1. Steady load

The steady load of the structure consisted of:

- the deadweight,
- the roof weight,
- the weight of elements hanged under the roof (light and sound systems, media screens and working platforms).

The deadweight was generated automatically in a calculation package; the roof weight (polycarbonate panels) was applied as superficial gravitational loading, and the hanging elements weight was modeled as concentrated force and linear load applied to corresponding structural elements. The weight of the technical fabric was omitted due to its negligible influence.

5.2. Technological load

The following were treated as technological load:

- load for structure by stretch of fabrics,
- operational load of a working platform.

Forces induced by the fabrics stretch were modeled as a simplified, constant in time, and applied directly on girder straps. The operational load was applied at corresponding attachment locations and was treated as linear.

5.3. Snow load

The snow load was modelled using methods that approximate the distribution of the forces for a nonstandard shape of structure's roof. The approximation was based on standards included in work [10]. The combination of guidelines for multi-hipped and wagon roofs was implemented.

5.4. Wind load

Wind load was determined analogically to snow one: using approximating methods based on guidelines included in standard [11]. The proposed solution allows for estimation of pressure distribution caused by wind action through adaptation of guidelines for typical structures. The wind load analysis frequently plays a key role during a design stage which is also reflected in research efforts, e.g., [1, 5, 7]. It is well known that for some engineering objects the gust wind can cause the excessive vibrations, deflections etc. The pressure coefficients obtained on the roof's surface for different directions of the wind are depicted in Figs. 14-17.

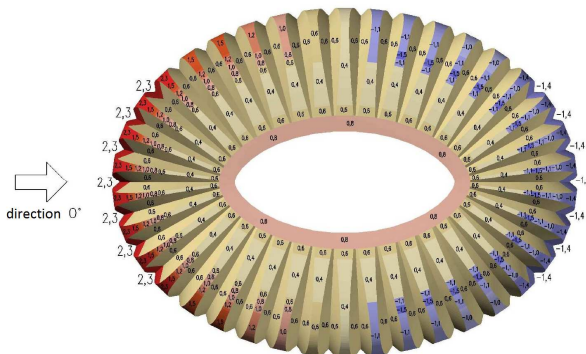


Fig. 14. Maximum pressure coefficients for wind at 0° angle.

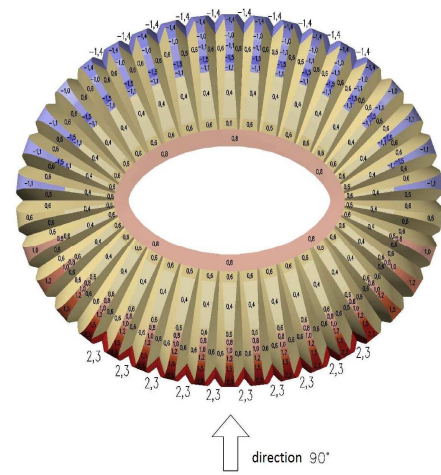


Fig. 15. Maximum pressure coefficients for wind at 90° angle.

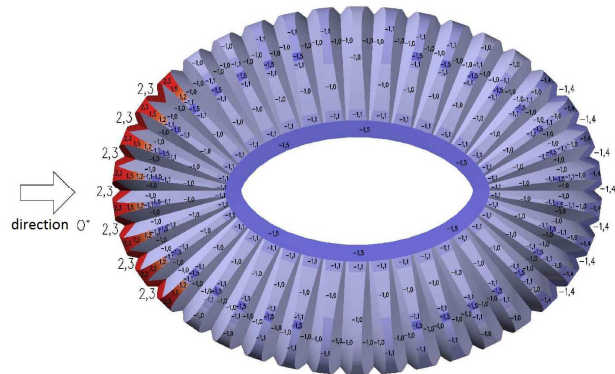


Fig. 16. Minimum pressure coefficients for wind at 0° angle.

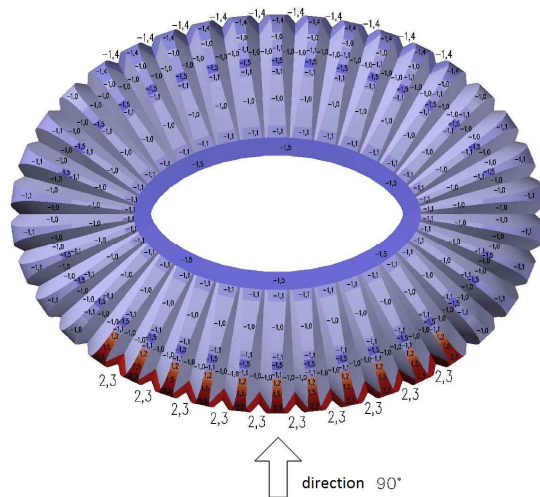


Fig. 17. Minimum pressure coefficients for wind at 90° angle.

A preview simulation of wind flow around the stadium's roof was conducted for the purpose of comparison. The software used for the simulation was Autodesk Flow Design: a tool used for a simplified air flow analysis similar to a wind tunnel. The obtained pressure maps for two wind directions are presented in Fig 18. It can be observed that, based on the simulation results, the pressure distribution obtained in such a way resembles minimum wind impact (based on [11]) most closely (Figs. 16-17). An analogy in pressure distribution can be noticed, particularly on the windward side of the object where the wind pressure is significant. Another value that stands out is the negative pressure at the flattened area of the roof's curvature which corresponds to coefficient pressure map created based on standards.

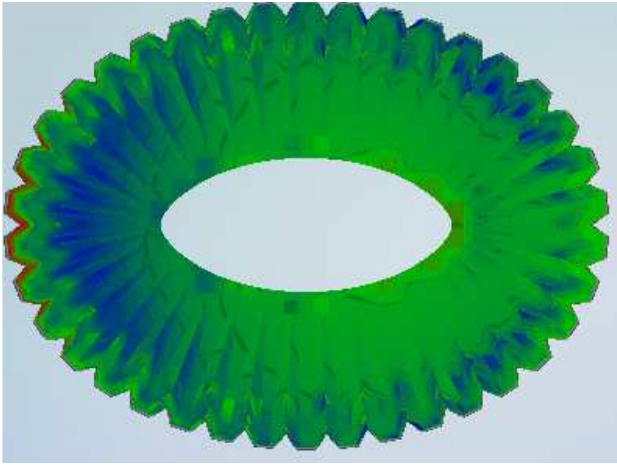


Fig. 18. Pressure map obtained from air flow simulation in software Autodesk Flow Design for 0° wind angle.

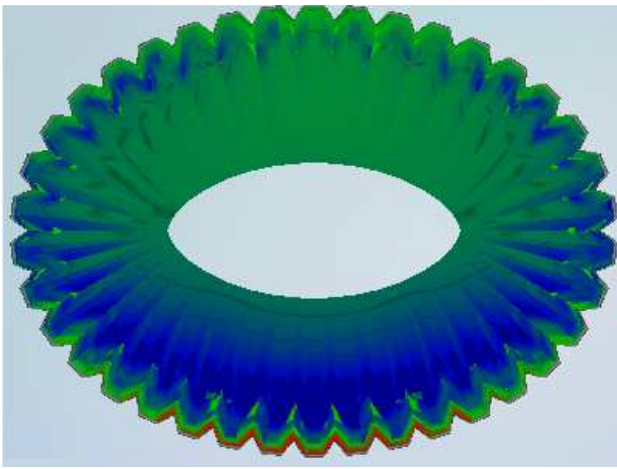


Fig. 19. Pressure map obtained from air flow simulation in software Autodesk Flow Design for 90° wind angle.

6. NUMERICAL ANALYSIS

6.1. Numerical analysis of a single girder

Linear statics was used for numerical calculations for a single girder model.

Sizing of bars from the analyzed structure were chosen according to three criteria:

- limiting slenderness ratio,
- minimum and maximum stress,
- maximum global displacement.

The condition for slenderness is presented in the relation:

$$\frac{L_{cr}}{i} \leq 200, \quad (4)$$

where:

L_{cr} – critical buckling length,

i – minimum radius of gyration of the cross-section.

It was assumed that the maximum allowed stress in the cross-section was yield point for construction steel $f_y=355$ MPa.

Global displacements of the structure was limited by:

- vertical displacements:

$$w_{max} \leq \frac{L}{250} = \frac{103,8 \text{ m}}{250} = 0,415 \text{ m}, \quad (5)$$

- lateral displacement:

$$v_{max} \leq \frac{H}{150} = \frac{40,9 \text{ m}}{150} = 0,273 \text{ m}, \quad (6)$$

where

L – double reach of the cantilever,

H – height of the structure.

Maximum deflection of girder's top node (Fig. 20) was obtained for a setting in which the primary variable action is snow load whereas the operational load and maximum wind at angle 0° are secondary. No characteristic setting exhibited structure's lifting. The least vertical displacement was 6.0 cm (Fig. 21) which could be found in a setting where the sole variable action was wind at 90° angle. A slightly higher displacement was found in a setting where the wind was of negative pressure at angle 0° - the lifting was 6.3 cm. The initial deflection caused by the fixed loading reached 20.8 cm.

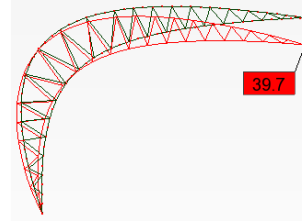


Fig. 20. Maximum deflection of a girder's node.

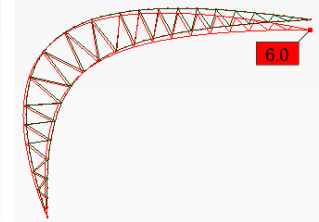


Fig. 21. Minimum deflection of a girder's node.

The wind's suction causes the reduction of displacement by as much as 14.8 cm while the displacement caused by the deadweight alone is only 20.8 cm. Taking this fact into consideration, it can be stated that the lifting impact of the wind on the structure is significant.

6.2. Numerical analysis of the roof

The structure model exhibits presence of bar densities which contributes to tension forces only. Therefore the calculations were performed with a nonlinear analysis based on iterations. 40 steps were established as an initial condition, but they were not enough to achieve coherent results of all load settings for such a number. The number of iterations was finally increased to 60 which allowed for effective calculations.

The maximum displacement of the structure (Fig. 22) was achieved for a setting where the primary action is the variable load of the maximal wind at 90°, while the operational load and the first case snow load are secondary.

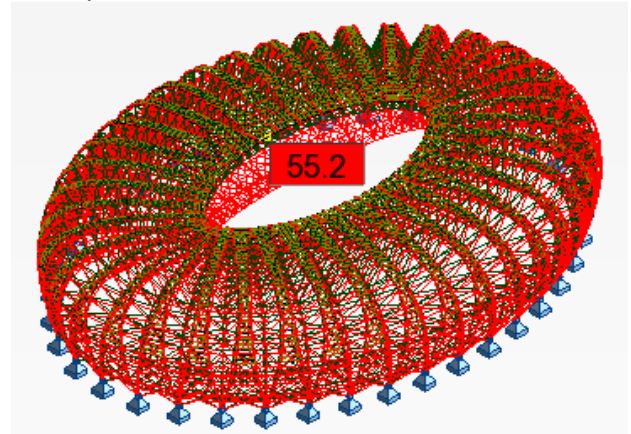


Fig. 22. Maximum structure displacement occurring at the node of the comparative girder (non-uniform scale).

The displacement values were as follows: the vertical displacement was 51.9 cm and the lateral one was 18.8 cm. Those values were noticed at the node of a girder located inside the longer axis of the ellipsis. No characteristic setting led to structure's lifting. The least displacement for the comparative girder was 12.7 cm (Fig 23) for the case where the minimal wind at 0° angle was the only variable load. Examining the

case globally, the lowest nodal displacement of all girders was achieved for the nodes located at the top ring of the structure, where the curvature is the greatest. The total value of this displacement was 6.3 cm for the setting with variable load represented by minimal wind at 0°.

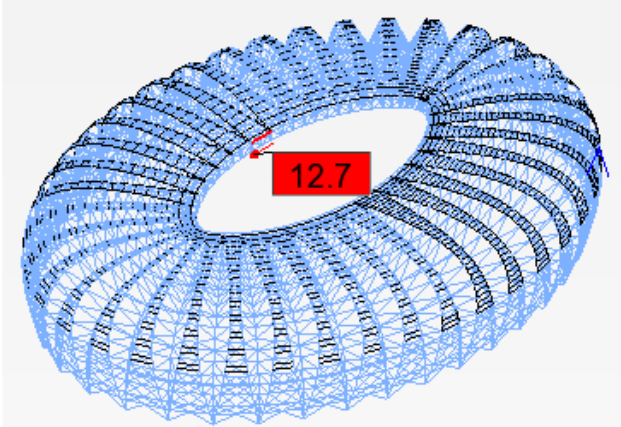


Fig. 23. Minimum structure displacement occurring at the node of the comparative girder (non-uniform scale).

Initial vertical displacement for fixed loading achieved maximum value of 22.7 cm located at the node of the comparative girder. Similar to the case of the single girder analysis, it was stated that the lifting impact of the wind on the structure is significant because it causes the decrease in displacement by 29.2 cm. When the obtained displacement values were compared against those for a single girder, it could be observed that the ones for the whole structure were greater, concerning both the maximum values and the lifting action of the wind.

The difference between the models was nearly 31 % which was caused by taking spatial modelling of all the elements of the structure in the second approach into consideration. A similar set of displacement could be observed for fixed loading. They were 20.8 cm and 22.7 cm for particular models. The difference in relation to the first one was therefore 9%.

6.3. Numerical analysis of a single girder with a changed static scheme of the structure

The above analyses indicate that the values of permitted displacement were exceeded. Their reduction was impossible without introducing changes to the geometry of the structure. Despite a change in elements' cross-sections and complying with criteria for slenderness and allowable stress, vertical displacement values did not change. An additional analysis of an altered structure's model was therefore conducted. The static scheme of the girders was altered in such a way that additional supporting elements were introduced along radial and vertical directions. The bottom straps of the girders were supported on the stands. Importantly, such a solution was implemented also in the real stadium, Beira Rio.

A fragment of the computational model with an additional supporting element is presented in Fig 24. The additional elements consist of a pillar and a strut each. It was modelled as a double articulated one, with fixed rotation around the axis of the pillar. The cross-sections of the elements were selected based on conditions defined in point 6.1. The analysis was conducted without a change in cross-sections of the elements in order to compare stress and displacement of the structure. The maximum displacement of the structure and stress in elements get significantly reduced with the additional support.

The maximum total displacement reached 34.0 cm, with the vertical component of 32.4 cm and the horizontal one of 8.0 cm. The values are smaller than those from the model without supporting elements by 38% and 57% consecutively.

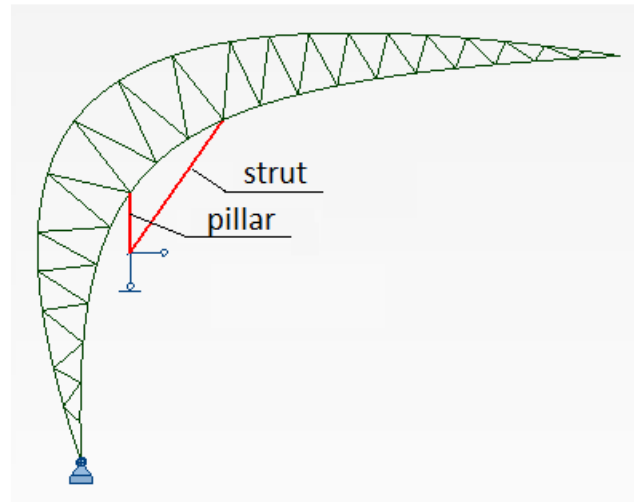


Fig. 24. A fragment of the structure's computational model with an additional supporting element (red).

The values of stress in elements were reduced by 20% on average while an increase in tensile stress was observed in case of minimal stress in girders' straps: 84% for the bottom strap and 9% for the top ones. The difference stems from the fact that the internal forces are transferred from the bars of supporting elements to the bottom straps and from the truss to top straps. It was also noticed that the extreme stress values in bottom straps of the girders are located at the additional supporting elements.

6.4. The impact of support susceptibility on the results of the analysis

Numerical calculations were performed for the model of the whole structure in order to find the impact of non-homogeneous soil below foundation level. The elasticity in vertical direction of the supporting elements, resulting from relationship for base of foundation [12]:

$$C = 2,50 \frac{E_0}{B(1+\nu^2)} \left[\frac{MN}{m^3} \right], \quad (7)$$

where

C – subsoil susceptibility coefficient,

E_0 – soil initial deformability modulus,

B – foundation width,

ν – Poisson's ratio.

The above parameters were defined based on standards [13]. The diversification of soil elasticity was achieved by assuming different soil types:

- medium sand of consolidation $I_D=0.7$,
- fine sand of consolidation $I_D=0.7$.

it was assumed that the object would be located on a foundation slab so the width of the foundation was set to the girder's reach, $B=15.5$ m, and the length of the object was set to $L=10.0$ m.

The coefficient of subsoil susceptibility for medium sand:

$$C_{Ps} = 2,50 \frac{110}{15,5(1+0,25^2)} = 17,0 \frac{MN}{m^3}, \quad (8)$$

The coefficient of subsoil susceptibility for fine sand:

$$C_{Pd} = 2,50 \frac{70}{15,5(1+0,30^2)} = 10,0 \frac{MN}{m^3}. \quad (9)$$

The subsoil elasticity coefficients (K_z) for a single-point supporting elements were calculated based on the above values in order to model the susceptibility by computational software

- for medium sand:

$$K_{z,Ps} = C_{Ps} \cdot B \cdot L = 17 \cdot 15,5 \cdot 10 = 2635000 \frac{kN}{m}, \quad (10)$$

- for fine sand:

$$K_{z,Pd} = C_{Pd} \cdot B \cdot L = 10 \cdot 15,5 \cdot 10 = 1550000 \frac{kN}{m}, \quad (11)$$

These coefficients were used as extreme ones for shaping of variability of elasticity coefficient of the supporting element in vertical direction. The distribution of elasticity coefficient was presented in Fig. 25. The red sections depict displacement (the lower the coefficient the greater the displacement of a supporting element). The calculations were performed for the whole structure model without additional supporting elements.

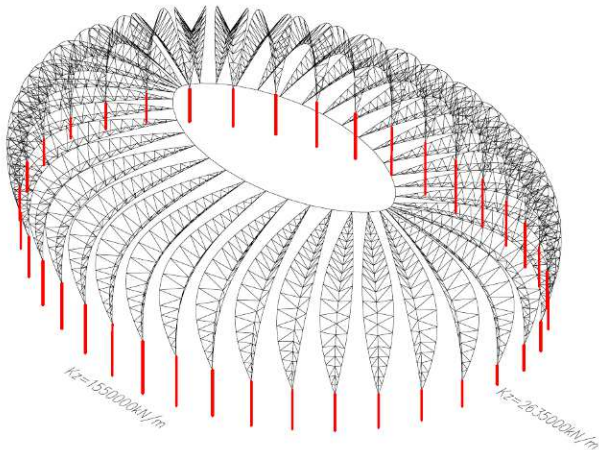


Fig. 25. Vertical elasticity coefficients distribution for supporting elements of the girders.

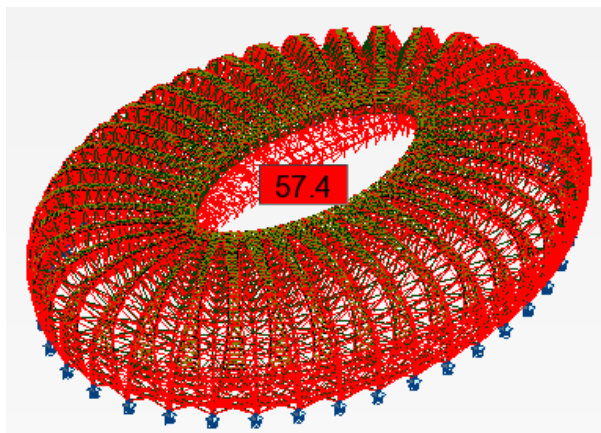


Fig. 26. The total displacement of the structure with susceptible supports.

The maximum vertical displacement of the supporting elements of coefficient equal to 1550000 kN/m could be observed during an analysis of the calculation results for the structure model with the assumed subsoil elasticity. However, they were barely 0.18 cm reaching double the value of settlement value for a minimum supporting element: 2635000 kN/m. Despite such small settlements resulting from the large size of the foundations, the strain of the whole structure and elements' stress increased. The total displacement for the structure was presented in Fig. 26. The vertical component was 53.9 cm and horizontal one was 16.5 cm. The vertical displacement increased by 4 % and the horizontal one decreased by 12 % in relation to the model of the supporting elements that were not susceptible. Similar differences were noticed in case of element stress. The greatest were 11 % for minimum stress in the inner ring of the truss ring and 8% for stresses in straps for bottom girders. Other stresses were increased by 3 % on average. The steel

elasticity limit was exceeded for the case of the outer truss ring and bracing rods.

Despite the slight displacement of vertical supporting elements the increase in both minimal and maximal stresses occurred in structure's elements. Whereas the increase was not big for the analysed case, it could lead to significantly stronger internal forces in case of greater differences in susceptibility of the soil.

7. CONCLUSIONS

This work elaborated on an attempt at taking a design approach from the existing Beira Rio stadium and adapting it in order to design a roof for a sports object intended for speedway competitions. The main aim was an analysis of the structure of roof's reach allowing for covering not only the stands but also the speedway tracks. The conducted research yielded the following conclusions:

- despite the large girder's reach (about 52.0 m), a static structure of the proposed geometry is possible. However, one negative result of such a large roof is a necessity for considerable height of the structure which is proportional to the reach of girders;
- the description of a structure with bracket and structural systems made by the authors is important for the analyzed case because the uniformly arranged arch girders were used where a fragment of a pillar and an element similar to bracket can be noticed. The stability, in turn, was guaranteed by spatial mating of all the girders and the rings connecting them;
- due to critical impact of climate-induced load on the structure's response, this type of load should be determined as accurately as possible to be a firm basis for computational analyses of nonstandard geometry objects;
- the approximation methods for determination of climate load accepted by the authors are not precise enough to create a design project of a real object on their basis, but form a basis performing initial calculations and examining global response of the structure based on its displacement or response direction of the supporting elements. In order to approximate the real climate-induced load better and verify the approximations made based on the standards, it would be necessary to conduct costly research in a wind tunnel;
- a computational analysis of a single girder yielded results which were not similar to the ones for the whole structure, that is, they resembled the other only for stress values in girders' straps. It is therefore not founded to determine the response of a bracket-structural object to loads based on a model of such a small fragment of the whole. In order to obtain reliable results, the analysis of the whole structure is necessary and the stiffness and mating of individual elements has to be taken into consideration because it is impossible to determine those relations without a spatial model for such a complex structure;
- keeping the limits of the allowed strain appeared to be the hardest condition to fulfill. Their criteria were exceeded by more than 10.0 cm for the whole structure model. A proposed solution of reducing the deflection by adding additional supporting elements achieved the expected goal reducing it by 38% in case of vertical displacement, but an increase in stress occurred in girders' straps at the same time. Moreover, a complete change in static scheme caused change in senses and values of support reactions. The object behaved more like a typical bracket structure.
- an important part of the analysis is taking into consideration a non-uniform susceptibility of the supporting elements as even small settlement values induce a noticeable increase in stress and total displacement of the structure.

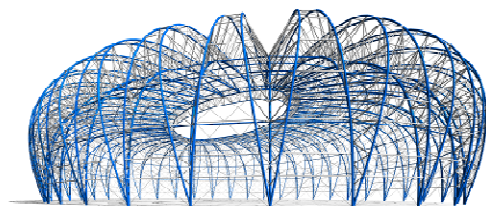


Fig. 27. General view of the analysed stadium's roof.

8. REFERENCES

1. Borrini C., Biagini., Structural response of large stadium roofs due to dynamic wind actions. *Stahlbau*, 74(3), 197-206, 2005.
2. Culley P., *Steel in Stadia*. *NSC Magazine*, Sport & Leisure, May 2002, Vol. 10, No.3.
3. Culley P., Pascoe J., *Sports facilities and technologies*, Rotledge, 2009, London.
4. Godycki-Ćwirko T., Trykosko R., Wojdak R., Żółtowski K., *Stadion piłkarski na Euro 2012 w Gdańsku Letnicy*, *Inżynieria i Budownictwo*, nr 10/2009 (in Polish).
5. Hoff van T., Blocken B., Harten van M., *3D CFD simulations of wind flow and wind-driven rain shelter in sports stadia: Influence of stadium geometry*. *Building and Environment*, 46(1), 22-37, 2011.
6. FIM Standards for track racing circuits (STRC) 2013.
7. Letchford C.W., Denon R.O., Johnson G., Mollam A., *Dynamic characteristics of cantilever grandstand roofs*. *Engineering Structures*, 24(8), 1085-1090, 2002.
8. PN-EN 13200-1:2007 – Obiekty widowiskowe. Część 1: Ogólna charakterystyka widowni (Polish standard).
9. PN-EN 13200-4:2007 – Obiekty widowiskowe. Część 4: Siedziska. Właściwości wyrobu (Polish standard).
10. PN-EN 1991-1-3:2005 – Actions on structures. Part 1-3: General actions – Snow actions.
11. PN-EN 1991-4:2004 - Actions on structures. Part 1-4: General actions – Wind actions.
12. Piętkowski R., *Foundation practice*, Arkady, Warszawa 1969 (in Polish).
13. PN-81/B-03020 – Grunty budowlane. Posadowienie bezpośrednie budowli. Obliczenia statyczne i projektowanie (Polish standard).